Geophysical Research Letters

Supporting Information for

Particle triggered reactions as an important mechanism of alkalinity and inorganic carbon removal in river plumes

E. Wurgaft[1,2], Z. A. Wang[1], J. H. Churchill[3], T. Dellapenna[4], S. Song[1,5], J. Du[6], M.C. Ringham[1,7], T. Rivlin[8,9] and B. Lazar[9]

[1]Department of Marine Chemistry and Geochemistry, Woods Hole Oceanographic Institution, Woods Hole, MA, USA.

[2]Avinoam Adam Department of Natural Sciences, The Israeli Open University, Ra'anana, Israel.

[3]Department of Physical Oceanography, Woods Hole Oceanographic Institution, Woods Hole, MA, USA.

[4]Department of Marine and Coastal Environmental Sciences, Texas A&M University at Galveston.

[5]State Key Laboratory of Estuarine and Coastal Research, East China Normal University,

Shanghai, China.

[6]Department of Applied Ocean Physics and Engineering, Woods Hole Oceanographic Institution, Woods Hole, MA, USA.

[7]Department of Earth, Atmosphere, and Planetary Sciences, Massachusetts Institute of Technology, Cambridge, MA, USA.

[8]Interuniversity Institute for Marine Sciences, The H. Steinitz Marine Biology Laboratory, The Hebrew University of Jerusalem, Eilat, Israel.

[9]Freddy and Nadine Herrmann Institute of Earth Science, The Hebrew University of Jerusalem, Jerusalem, Israel.

Corresponding author: Eyal Wurgaft (wurgaft@openu.ac.il)

Contents of this file

Introduction

This supplementary file includes data that support the main article, entitled "Particle triggered reactions as an important mechanism of alkalinity and inorganic carbon removal in river plumes". The raw data used for the calculations included in the main text and described here are available at https://www.bco-dmo.org/dataset/821117.

Text S1. Carbonate system, nutrients and major ions bottle sampling and sample analyses

Seawater samples acquired to determine carbonate system parameters were filtered through a 0.45 µm capsule filter into 250 ml Pyrex borosilicate glass bottles, poisoned with 100 µL of saturated $HgCl_2$ solution, and then sealed either with greased ground-glass stoppers or HDPE screw caps with a gas seal lining. Following the carbonate system parameter sampling, seawater was transferred into 15 mL and 60 mL centrifuge vials for nutrients and major ions analysis, respectively. These samples were acidified with 100 µL of HCl (0.1 N) and were kept in the dark at 4 °C until their analysis.

Total alkalinity (TA) was measured by a modified, open-cell, potentiometric Gran titration *[Wang and Cai*, 2004], using an Apollo Sci Tech automated titrator (AS-ALK2). Titrations were conducted at a controlled temperature (22 °C), using HCl 0.07 M as titrant. The HCl concentration was determined at the beginning and the end of each analytical session by titrations of Certified Reference Material (CRM) provided by Dr. A.G. Dickson at the Scripps Institution of Oceanography. Each sample was measured twice. The precision of the TA measurements (mean difference between duplicate measurements with one standard deviation) was 0.4 ± 0.2 µmol kg^{-1}. The measured TA of the CRM at the end of each session was within ± 1.2 µmol kg^{-1} of the reported value, which was treated as the total error of TA measurements. Dissolved inorganic carbon (DIC) was measured by an automatic analyzer (AS-C3, Apollo Sci Tech) attached to a non-dispersive infrared analyzer (LICOR 7000), which was calibrated by measurement of varying volumes of CRM at the beginning and at the end of each analytical session [*Wang and Cai*, 2004; *Wang et al.*, 2017]. The DIC precision, based on duplicate measurements, was better than ± 2 µmol kg^{-1}. Sample pH was measured spectrophotometrically, using purified m-cresol purple indicator [*Dickson et al.*, 2007; *Liu et al.*, 2011]. The precision of the measurement, based on duplicate measurements, was

better than ±0.001. The agreement between measured and calculated pH was better than ± 0.005 pH units. The calculation of pH from TA and DIC was done using the CO_2sys software by [*Pierrot et al.*, 2006; *Xu et al.*, 2017] with carbonate dissociation constants from [*Mehrbach et al.*, 1973] as fitted by *Dickson and Millero* [1987].

Dissolved inorganic nitrogen (DIN=NO_3+NO_2), silica and soluble reactive phosphate (SRP) concentrations were measured colorimetrically [*Grasshoff et al.*, 2009] using a flow injection analyzer (LACHAT Instruments Quick-Chem-8500). The internal precisions of the measurements were 0.05, 0.05 and 0.03 µmol l^{-1} for DIN, silica and SRP, respectively. High concentration solutions from commercial standard reagents (Merck) were diluted into a suite of solutions, which were used to calibrate the measurement.

The concentrations of the major ions (Na^+, Cl^-, Mg^{2+}, Ca^{2+}, K^+ and Sr^{2+}) were measured by an inductively coupled plasma mass-spectrometer (Agilent 7500cx) with precision of 0.5% of their respective concentrations.

The Org-Alk in selected samples was measured according to [*Cai et al.*, 1998; *Song et al.*, 2020]. Briefly, seawater was titrated to pH < 3. The sample was then bubbled with high purity N_2, and the pH was increased to its initial value by addition of CO_2-free NaOH. Thereafter, the sample was titrated a second time, using a modified Gran titration. The Org-Alk was calculated by subtracting the boric alkalinity from the result of the CO_2-free 2nd titration. Silicate and phosphate alkalinity was less than 1 µmol kg^{-1} (based on measured silicate and phosphate concentrations and pH values) and thus was ignored in the Org-Alk calculation. The precision of the NCA measurement, based on duplicate measurements, was better than ±4 µmol kg^{-1}.

Text S2. Seeding Experiments

Seawater for the seeding experiments was collected from the surface of the stations of the Mississippi and Brazos transects furthest away from the river mouths (Fig. 1). The water was filtered through a 0.45 µM filter and poisoned with saturated $HgCl_2$ (0.4 ml l^{-1}). The particles for the experiments were collected from the upper 5 cm of sediment cores collected near the river mouths. The particles were dried at 60 °C for 48 hours, and were then homogenized by grounding with mortar and pestel. The experiments were done in screw-cap Pyrex borosilicate bottles, in which 100 ml of seawater were seeded with 0.4 g of particles. A set of unseeded seawater bottles was used as control in each experiment. The water temperature recorded during the experiment was 21 ± 1 °C. At each sampling point, the seawater from two seeded bottles and two control bottles was filtered through a 0.2 µM filter into 30 ml screwcap Pyrex bottles (for DIC) and 30 mL plastic syringes (for TA) for sample analysis. The agreement in TA and DIC between the duplicate bottles at each time point was better than ± 6 µmol kg^{-1}.

Text S3. Assessment of particle-induced heterogeneous reactions

In this study, the overall deviations of TA and DIC from the river-ocean conservative mixing lines in the Mississippi and Brazos River plumes resulted from the following processes: net community production (photosynthesis - respiration), sediment input, biogenic $CaCO_3$ production, air-sea CO_2 exchange and heterogeneous interactions

with suspended particles. The TA and DIC deviations due to heterogeneous reactions were evaluated as the difference between the overall deviations from conservative mixing and the deviations from other processes:

$$(S1)\Delta TA_{HET} = TA_{OBS} - TA_{CON} - \Delta TA_{OTH}$$

$$(S2)\Delta DIC_{HET} = DIC_{OBS} - DIC_{CON} - \Delta DIC_{OTH}$$

where the Δ is deviation from conservative mixing between the river-mouth and open-sea endmembers (Table S1). The subscript "HET" denotes heterogeneous interactions, "OBS" is the observed concentration, and "CON" is the expected concentration from conservative mixing. The subscript "OTH" accounts for the processes other than heterogeneous interactions and conservative mixing:

$$(S3)\Delta TA_{OTH} = \Delta DIN + \Delta SRP - \Delta Org\text{-}Alk + 2\Delta CaCO_{3,BIO} + \Delta TA_{SED}$$

$$(S4)\Delta DIC_{OTH} = 5\Delta DIN + \Delta DIC_{air-sea} + \Delta DIC_{CaCO3,BIO} + \Delta DIC_{SED}$$

where ΔDIN, ΔSRP, and ΔOrg-Alk are the deviations of DIN, SRP and organic alkalinity from their respective conservative mixing lines, $\Delta CaCO_{3,BIO}$ is DIC removal by biogenic $CaCO_3$ production, ΔTA_{SED} and ΔDIC_{SED} are the seawater-sediment fluxes of TA and DIC, respectively, and $\Delta DIC_{air\text{-}sea}$ is the change in DIC due to air-sea CO_2 exchange. The Redfield ratio of 5 between DIC and DIN was used to convert ΔDIN to ΔDIC due to net community production, as reported by *Huang et al*. [2012].

Table S2 summarizes all assessed terms in equations 3 and 4. As there are no specific published estimates of $\Delta CaCO_{3,BIO}$ in either the Mississippi or the Brazos plume, we assumed a rate of 25 mmol C m^{-2} d^{-1}, which lies between estimates for continental shelf rates [*Smith*, 1972] and a rates typical for coral reefs [*Langdon et al.*, 2000]. In view of the absence of foraminifera and coccolithophore skeletons in the filtered sediment samples, we contend that this value is likely to be an overestimation of the actual $\Delta CaCO_{3,BIO}$. In either case, because of the short residence time of water in the two plumes (see Text S4), $\Delta CaCO_{3,BIO}$ has limited effect on ΔTA_{HET} and ΔDIC_{HET}. ΔTA_{SED} and ΔDIC_{SED} were taken from *Berelson et al.*, [2019]. The CO_2 exchange flux was calculated from measured pCO_2 difference between surface seawater and air together with the measured mean wind speeds during the sampling period in each plume. The parametrization of gas transfer velocity was calculated according to *Wanninkhof* [2014].

To estimate the changes in TA and DIC concentrations resulting from $\Delta CaCO_{3,BIO}$, ΔTA_{SED} , DIC_{SED} and $\Delta DIC_{air\text{-}sea}$, we calculated the travel time from the river end-member to each sampling point using the shipboard-ADCP velocity data. Notably, due to the short residence time (~2 days;Text S4) of water in the both river plumes, CO_2 exchange, biogenic $CaCO_3$ production and sediment input were all relatively minor terms compared to the effects of heterogeneous reactions.

Text S4. Assessment of water residence time in the river plumes

Given the possibility of temporal changes in the TA and DIC of the Mississippi and Brazos river endmembers, a potential uncertainty in interpreting the results shown in Figures 2 and 3 is the transit time or residence time (time since emergence from the river

mouth) of the plume water relative to the temporal scales of changes in riverine endmembers. If the residence time of plume water is long relative to the timescale of the riverine TA and DIC changes, then the variability of the riverine endmembers may cause errors of assessing the deviations of TA and DIC from conservative mixing [Officer, 1979].

Brazos River Plume – Estimation of the residence time of the water in the Brazos river plume (predominately in the 15-20 salinity range, Figure 3) is, to some extent, simplified by the nearfield configuration of the plume. The near-surface salinity data show the Brazos River plume taking the form of a coastal current extending to the southwest of the river mouth (Figure S6). This is consistent with the form of the plume as seen in the corrected surface reflectance (true color) field of September 10, 2017 (from NASA Worldview, Figure S7). The reflectance field, which is sensitive to the near-surface turbidity signal of a river plume (e.g., *Miller and McKee*, 2004), shows the plume turning abruptly to the right (southwest) upon emerging from the river mouth and subsequently confined to a narrow coastal region in the sampling area (Figure S7). Because water velocities in the Brazos plume are uniformly directed alongshore to the SW (Figure S6), the residence time of the plume water can be reasonably approximated by its alongshore travel time after emerging from the river mouth. To determine the timescale of plume water transport in the sampling region, we estimated transit time of water moving along a station transect that was contained within the plume and spanned the alongshore extent in the sampling region (Figure S6). The transit time between a station pair of the transect was estimated by dividing the distance between stations by their mean near-surface velocity . The estimated time of transit across the plume is ~8 hrs.

This result is consistent with the residence time of the Brazos plume determined by simulating the transit of drifters released from the mouth of the Brazos River based on a regional hydrodynamic model. The model has a domain covering the entire Texas, Louisiana, Mississippi, and Alabama coasts, including the shelf area as well as all major estuaries (e.g., Galveston Bay, Brazos River). It has been well calibrated in terms of water levels, temperatures, salinities and shelf currents on the Texas-Louisiana shelf and in Galveston Bay [*Du et al.*, 2019; *Du and Park, 2019*]. During the simulation, drifters were released into the model flow field at 131 closely spaced locations within the Brazos River and near the river mouth at hourly intervals between September 9 and 10, 2017. Using the drifter tracks, the residence time of each sampling station was estimated as: 1) defining a 'watch circle' around each station, and 2) averaging the transit time (time since release in the Brazos) of all drifters that passed through the circle at the time of the sampling within ±1/2 hr. The estimated residence time showed a similar progression along the station transect to the SW of the Brazos River mouth as determined by the ADCP data. The residence time at the most SW station exceeded that of the station closest to the Brazos River mouth by roughly 8 hr.

As such, both the model-drifter-based analysis and the calculations based on ADCP data indicate that the residence time of plume water was on the order of 8 hrs. As this is comparable with the time taken to survey the Brazos plume, we conclude that temporal changes in the TA and DIC of the Brazos River water were not a significant source of error in our analysis.

Mississippi River Plume – The surface reflectance imagery indicates that the Mississippi River plume had a shape of a bulge extending offshore, rather than a coastally bound flow, during the time of our sampling. Because a clear unidirectional flow structure was not observed in this 'bulge' plume structure by our shipboard ADCP data, estimating the residence time of the Mississippi plume using ADCP data and the approach described above is not a viable option. However, information on the plume residence time was discussed by *Lohrenz et al.* [1990] and *Hitchcock et al.* [1997]. *Hitchcock et al.* [1997] conducted two sets of studies (in May and August 1993) in which salinity and other water properties were measured in the Mississippi River plume along the paths of drifters released near the river mouth. The data revealed an increase in the salinity of the water tagged by the drifters from riverine values to 20-25 over a 24-hr period. This is generally in line with the estimated mean plume residence time of ~2 d by *Lohrenz et al*. [1990] using a mass balance calculation. Based on these prior studies, a residence time of 1-2 days for the Mississippi River plume was chosen for the analysis of this study.

Text S5. Error analysis

The errors of ΔDIC_{HET} and ΔTA_{HET} were estimated by propagating the errors of the terms in equations 1-4 in the main text. These errors and their estimates (Table S2) are described below..

5.1 Errors of the differences between measured and conservative mixing values The errors of the differences between the expected (from conservative mixing) and measured values of TA, DIC, DIN and SRP (Equations 1-4) result from the analytical errors of the measured values as well as the uncertainties of the conservative mixing lines. The former has been documented in Text S1. The latter stem from the errors of both endmembers, as illustrated in Figure S8, and as such depends on endmember salinity, TA and DIC.

One may expect that the uncertainties of endmember TA and DIC are largely due to temporal changes in riverine TA and DIC as the variability of the seawater endmember is relatively insignificant [*Cai*, 2003; *Guo et al.*, 2012; *Huang et al.*, 2012; *Officer*, 1979]. If the changes of the river endmember occur over a shorter time scale than the residence time of water sampled in the plume, then the TA and DIC endmembers may not properly represent the TA and DIC of a given parcel of plume water when it emerged from the river mouth. To estimate the rate of TA and DIC change in the Brazos and Mississippi Rivers, we used the USGS data from site 07374525 (Belle Chasse, LA) for the Mississippi and site 0811650 (Rosharon, TX) for the Brazos. We assumed that the change occurred linearly between consecutive measurements. The change in DIC, which was not measured by the USGS, can be treated the same as the changes in TA since most TA in river water is predominantly in the form of bicarbonate [Cai et al., 2003]. We considered the product of the linear rate of TA change between two USGS measurements of a given river and the residence time of that river plume (see Text S4) as the variability or uncertainty of the riverine endmember. This uncertainty was added to the analytical error to yield the overall errors of the endmembers used for the calculation of the values on

the conservative mixing lines. Then, the error of the differences between the conservative and the measured TA and DIC values were calculated from the differential of the subtraction function, showed here for TA:

$$(S5)\quad e(TA_{OBS} - TA_{CON})_{(S)} = \sqrt{\left(eTA_{OBS,S}\right)^2 + \left(eTA_{CON,S}\right)^2}$$

where *e* represents the error in concentration units. The errors of ΔDIN, ΔSRP and ΔOrgAlk were calculated in the same manner. As mentioned above, the error of these differences is a function of the salinity. However, for the sake of simplicity, we used the maximal error of each parameter along the entire salinity gradients, ±5 and ±6 μmol kg^{-1} for TA and DIC, respectively.

5.2 Errors of ΔTA_{OTH} and ΔDIC_{OTH}

Errors of the flux terms in Equations S3 and S4, including $\Delta CaCO_{3,BIO}$, ΔTA_{SED}, ΔDIC_{SED} and $\Delta DIC_{air\text{-}sea}$, were assessed based on the uncertainty associated with each flux term and the residence times in each system. The error of $\Delta CaCO_{3,BIO}$, was estimated based on the uncertainty of the range of $CaCO_3$ production rates considered here (10-40 mmol C m^{-2} d^{-1}, see Text S3). The error of ΔTA_{SED} and ΔDIC_{SED} was determined based on the range of values presented in the study by Berelson et al. [2019].. The error of $\Delta DIC_{air\text{-}sea}$ was estimated as 30%, based on the uncertainty associated with the parameterization of wind-speeds to gas-exchange coefficients [*Wanninkhof*, 2014].

The errors of ΔDIN, ΔSRP and ΔOrgAlk and the above-mentioned errors of the flux terms were used to calculate the errors of ΔTA_{OTH} and ΔDIC_{OTH}, which amounted to 16 μmol kg^{-1} for both terms.

5.3 Errors of ΔTA_{HET} and ΔDIC_{HET}

The errors of the differences between conservative and measured DIC and TA values (Equation S5) and the errors of ΔTA_{OTH} and ΔDIC_{OTH} were used to estimate the overall errors of ΔTA_{HET} and ΔDIC_{HET}. The main contribution to the overall error comes from the uncertainty of the river endmember concentration. The uncertainty decreases with increasing salinity, to a local minimum at S~25. However, for the sake of simplicity, we applied the maximal error to all of our calculations. Consequently, the estimated total error of ΔTA_{HET} and ΔDIC_{HET} is ±17 μmol kg^{-1}.

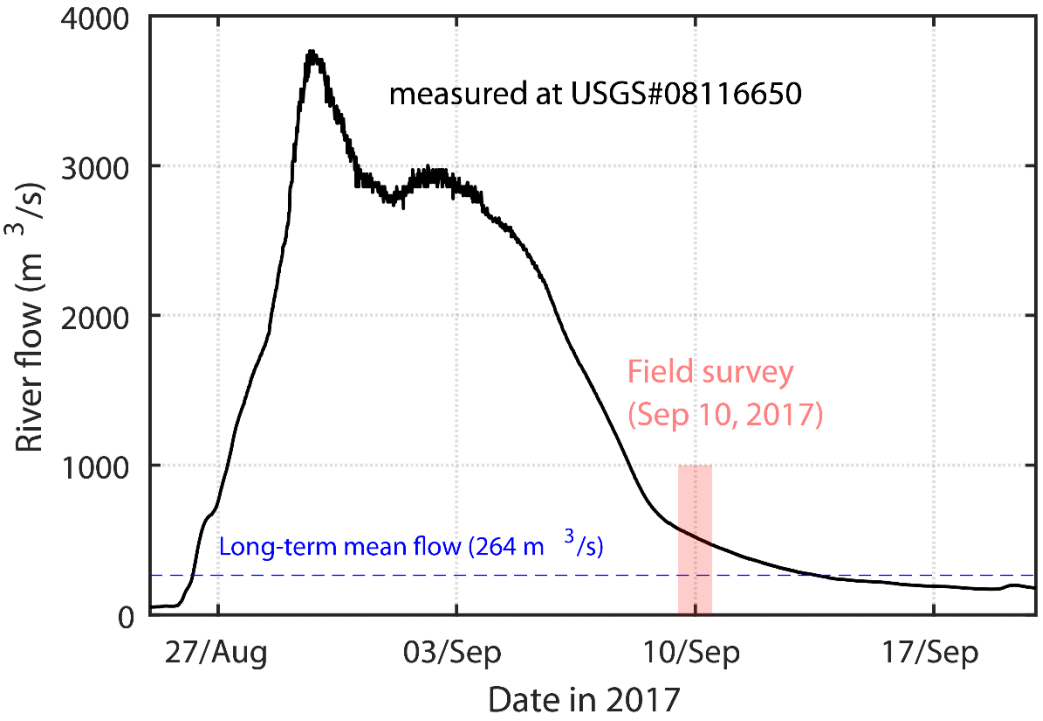

Figure S1. Freshwater discharge of the Brazos River during Hurricane Harvey.

Figure S2. A photograph showing the particle-laden plume of the Brazos River. The extra high-turbidity river plume is the result of the flooding following Hurricane Harvey, which

made landfall on the shore of Texas and the Brazos drainage basin on August 26, 2017, about two weeks prior to the sampling cruise of this study (9-18 September 2017).

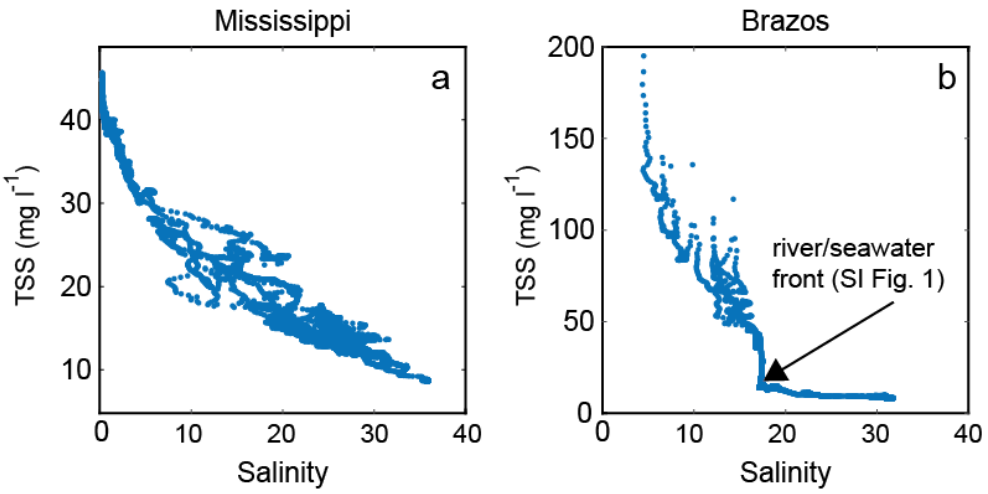

Figure S3. TSS vs salinity in the plumes of the Mississippi (a) and Brazos (b) Rivers. Note the sharp increase in TSS at S~17 in the Brazos river plume. This increase corresponds to the visible front seen in Figure S2.

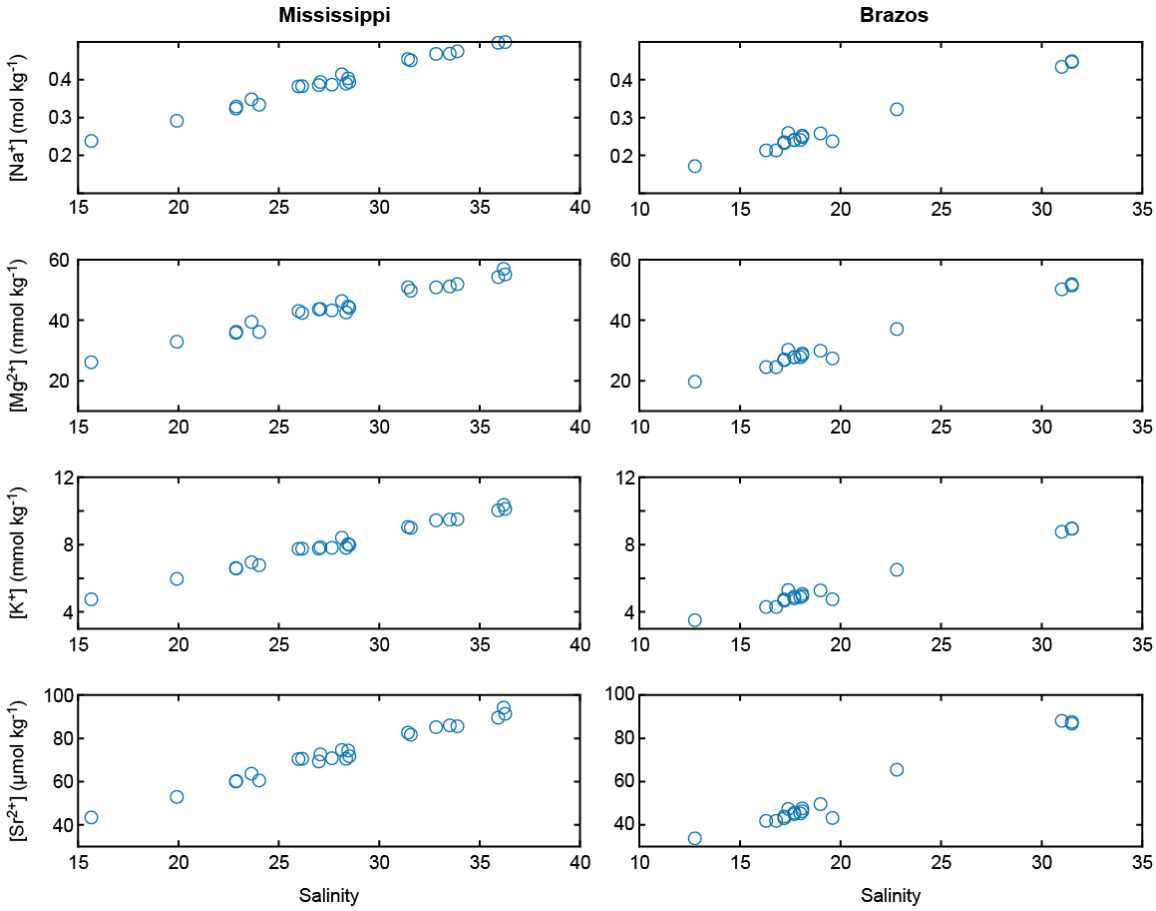

Figure S4. The distribution of major ions (Na^+, Mg^{2+}, K^+ and Sr^{2+}) along the salinity gradient in the plumes of the Mississippi (panels on the left column) and Brazos (right column) Rivers.

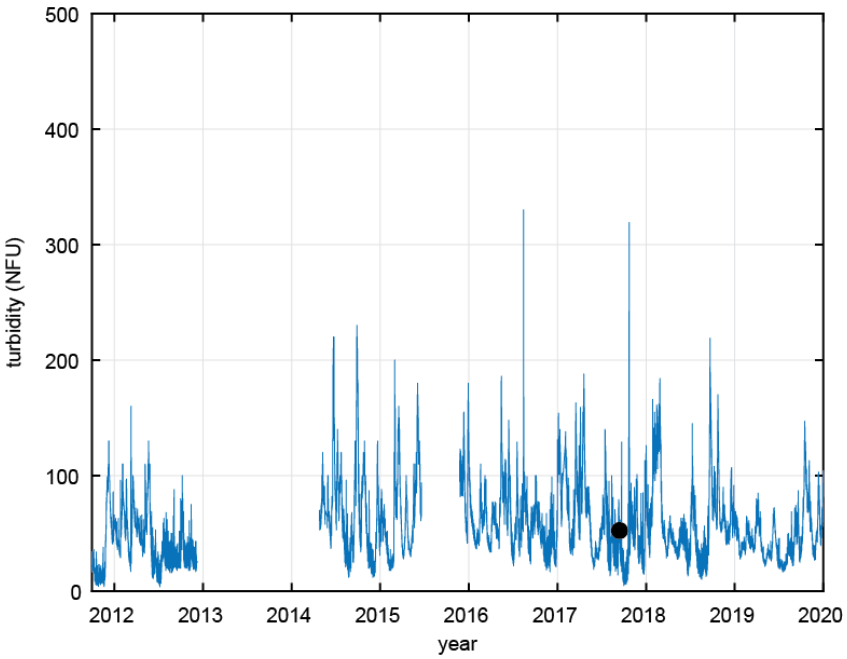

Figure S5. Time-series turbidity record at the USGS gauge station 07374000 near Baton Rouge, Louisiana. The black circle shows the period of the field sampling in this study.

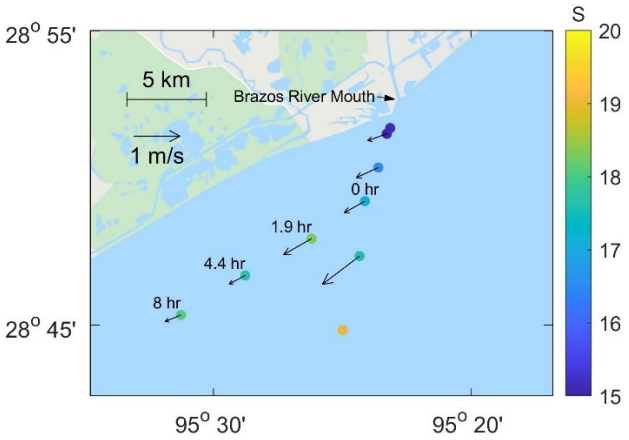

Figure S6. Measurements of near-surface salinity (S) and water velocity at 5.5 m (averages of all ADCP data taken at each circled CTD station) in the Brazos River plume on September 10, 2017. The velocity measurements at the seaward most station (yellow circle) were missing.

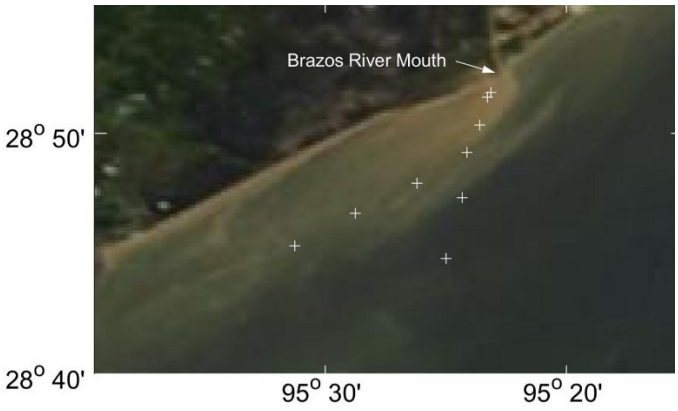

Figure S7. The corrected surface reflectance (true color) field from September 10, 2017 (NASA Worldview; https://worldview.earthdata.nasa.gov/) overlaid with the CTD stations (crosses) in the Brazos River plume. Note the high turbidity plume of the Brazos River (light-brown coloring) turning abruptly to the right along the flow path after emerging from the river mouth and continuing to the southwest as a trapped feature of suspended particles.

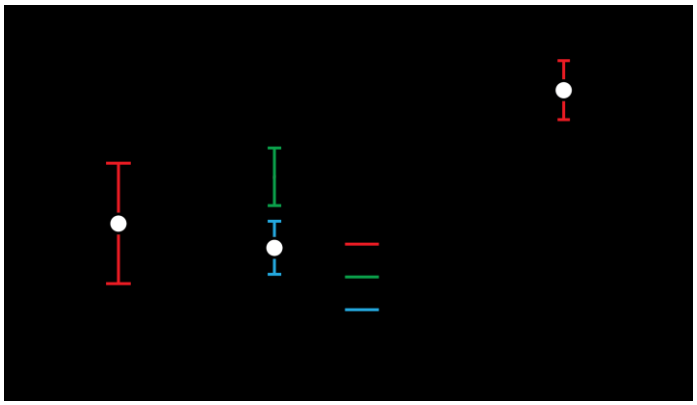

Figure S8. Schematic of the error analysis for the two-endmember mixing model. The error of the mixing line results from the error margins of the two endmembers (red vertical lines), which was calculated as the difference between the upper and lower boundaries (dashed lines) around the mixing line (black line). The error of the mixing line at a specific salinity (green vertical line) was added to the analytical error of the data at the same salinity (blue vertical line), the sum of which represent the total error when calculating the deviation from the mixing line (Equations S1-S4).

Table S1. River-mouth and open-sea endmembers.

River	endmember	S	TA	DIC	DIN µmol kg^{-1}	SRP	Org-Alk
Mississippi	river mouth	15.66	2452	2424	76.33	3.80	38
	open-sea	36.19	2390	2159	6.34	0.46	55
Brazos	river mouth	13.93	1827	1794	3.85	2.62	136
	open-sea	31.33	2345	2028	0.20	0.23	118

. **Table S2.** TA, DIC flux terms and residence times used to calculate ΔTA_{HET} and ΔDIC_{HET} (Equations S3 and S4).

	Mississippi	Brazos	maximal effect on concentration	Ref.
	mmol m^{-2} day^{-1}		µmol kg^{-1}	
$\Delta CaCO_{3,BIO}$	-25±15	-25±15	5±7	[*Langdon et al.*, 2000; *Smith*, 1972]
ΔTA_{SED}	40±20	40±20	5±11	[*Berelson et al.*, 2019]
ΔDIC_{SED}	40±20	40±20	7±11	
$\Delta DIC_{air\text{-}sea}$	-53±18	-130±143	13±9	[*Wanninkhof*, 2014]
residence time (day)	2±1	0.3±0.2		This study (calculated from ADCP and drifter data)

References:

Berelson, W. M., J. McManus, S. Severmann, and N. Rollins (2019), Benthic fluxes from hypoxia-influenced Gulf of Mexico sediments: Impact on bottom water acidification, *Marine Chemistry*, *209*, 94-106.

Cai, W. J. (2003), Riverine inorganic carbon flux and rate of biological uptake in the Mississippi River plume, *Geophysical Research Letters*, *30*(2).

Cai, W. J., Y. C. Wang, and R. E. Hodson (1998), Acid-base properties of dissolved organic matter in the estuarine waters of Georgia, USA, *Geochimica Et Cosmochimica Acta*, *62*(3), 473-483.

Cai, W. J., X. P. Hu, W. J. Huang, L. Q. Jiang, Y. C. Wang, T. H. Peng, and X. Zhang (2010), Alkalinity distribution in the western North Atlantic Ocean margins, *Journal of Geophysical Research-Oceans*, *115*.

Dickson, A. G., C. L. Sabine, and J. R. Christian (2007), *Guide to Best Practices for Ocean CO_2 Measurements*, PICES special publication.

Du, J., & Park, K. (2019). Estuarine salinity recovery from an extreme precipitation event: Hurricane Harvey in Galveston Bay. *Science of The Total Environment*, 670, 1049–1059.

Du, J., Park, K., Shen, J., Zhang, Y. J., Yu, X., Ye, F., et al. (2019). A hydrodynamic model for Galveston Bay and the shelf in the northern Gulf of Mexico. *Ocean Science*, 15(4), 951–966.

Grasshoff, K., K. Kremling, and M. Ehrhardt (2009), *Methods of seawater analysis*, John Wiley & Sons.

Green, R. E., T. S. Bianchi, M. J. Dagg, N. D. Walker, and G. A. Breed (2006), An organic carbon budget for the Mississippi River turbidity plume and plume contributions to air-sea CO 2 fluxes and bottom water hypoxia, *Estuaries and Coasts*, *29*(4), 579-597.

Guo, X., W.-J. Cai, W.-J. Huang, Y. Wang, F. Chen, M. C. Murrell, S. E. Lohrenz, L.-Q. Jiang, M. Dai, and J. Hartmann (2012), Carbon dynamics and community production in the Mississippi River plume, *Limnology and Oceanography*, *57*(1), 1-17.

Huang, W.-J., W.-J. Cai, R. Powell, S. Lohrenz, Y. Wang, L.-Q. Jiang, and C. Hopkinson (2012), The stoichiometry of inorganic carbon and nutrient removal in the Mississippi River plume and adjacent continental shelf, *Biogeosciences*, *9*(7), 2781-2792.

Langdon, C., T. Takahashi, C. Sweeney, D. Chipman, J. Goddard, F. Marubini, H. Aceves, H. Barnett, and M. J. Atkinson (2000), Effect of calcium carbonate saturation state on the calcification rate of an experimental coral reef, *Global Biogeochemical Cycles*, *14*(2), 639-654.

Liu, X. W., M. C. Patsavas, and R. H. Byrne (2011), Purification and Characterization of meta-Cresol Purple for Spectrophotometric Seawater pH Measurements, *Environmental Science & Technology*, *45*(11), 4862-4868.

Mehrbach, C., Culberso.Ch, J. E. Hawley, and Pytkowic.Rm (1973), Measurement of Apparent Dissociation Constants of Carbonic Acid in Seawater at Atmospheric Pressure, *Limnology and Oceanography*, *18*(6), 897-907.

Officer, C. B. (1979), Discussion of the behaviour of nonconservative dissolved constituents in estuaries, *Estuarine and Coastal Marine Science*, *9*(1), 91-94.
Pierrot, D., E. Lewis, and D. W. R. Wallace (2006), MS Excel Program Developed for CO2 System Calculations, edited, Carbon Dioxide Information Analysis Center, Oak Ridge National Laboratory, Oak Ridge.
Smith, S. (1972), Production of calcium carbonate on the mainland shelf of southern California 1, *Limnology and Oceanography*, *17*(1), 28-41.
Song, S., Z. A. Wang, M. E. Gonneea, K. D. Kroeger, S. N. Chu, D. Li, and H. Liang (2020), An important biogeochemical link between organic and inorganic carbon cycling: Effects of organic alkalinity on carbonate chemistry in coastal waters influenced by intertidal salt marshes, *Geochimica et Cosmochimica Acta*, *275*, 123-139.
Wang, Z. A., and W. J. Cai (2004), Carbon dioxide degassing and inorganic carbon export from a marsh-dominated estuary (the Duplin River): A marsh CO2 pump, *Limnology and Oceanography*, *49*(2), 341-354.
Wang, Z. A., G. L. Lawson, C. H. Pilskaln, and A. E. Maas (2017), Seasonal controls of aragonite saturation states in the Gulf of Maine, *Journal of Geophysical Research: Oceans, 122*(1), 372-389, doi: 10.1002/2016jc012373.
Wanninkhof, R. (2014), Relationship between wind speed and gas exchange over the ocean revisited, *Limnology and Oceanography: Methods*, *12*(6), 351-362.
Wawrik, B., and J. H. Paul (2004), Phytoplankton community structure and productivity along the axis of the Mississippi River plume in oligotrophic Gulf of Mexico waters, *Aquatic Microbial Ecology*, *35*(2), 185-196.

Xu, Y. Y., D. Pierrot, and W. J. Cai (2017), Ocean carbonate system computation for anoxic waters using an updated CO2SYS program, *Marine Chemistry*, *195*, 90-93.